Journal of Structural Geology 30 (2008) 1005–1012

Contents lists available at ScienceDirect

Journal of Structural Geology

journal homepage: www.elsevier.com/locate/jsg

Structural analysis of mylonitic rocks in the Cougar Creek Complex, Oregon–Idaho using the porphyroclast hyperbolic distribution method, and potential use of SC′-type extensional shear bands as quantitative vorticity indicators

Gene A. Kurz*, Clyde J. Northrup

Department of Geosciences, Boise State University, 1910 University Drive, Boise, ID 83725, USA

ARTICLE INFO

Article history:
Received 7 February 2007
Received in revised form 2 April 2008
Accepted 6 April 2008
Available online 18 April 2008

Keywords:
Vorticity
Shear Bands
Mylonites
Blue Mountains
Arc Terranes
Cougar Creek Complex
Oregon

ABSTRACT

Mylonitic rocks of the Cougar Creek Complex of northeastern Oregon and west-central Idaho provide an opportunity to document the deformational structures produced during general non-coaxial shear within quartz-feldspar mylonites and to explore the potential role of SC′-type extensional shear bands in vorticity analysis. Well-developed feldspar porphyroclasts within six mylonite zones were utilized to estimate bulk kinematic vorticity (W_k) using the porphyroclast hyperbolic distribution (PHD) method. W_k values for the Cougar Creek mylonites range from $W_k = 0.26$ to $W_k = 0.37$. Synthetic and antithetic shear band inclinations were measured relative to observed shear zone boundaries within five mylonite zones with estimated W_k values and compared to the non-coaxial flow field geometries and eigenvector orientations. In each mylonite zone, synthetic SC′-type shear band populations exhibit a range of inclination with maximum inclination lying approximately parallel to the acute bisector (AB) of the eigenvectors. Similarly, antithetic shear band populations show a range of inclination near the obtuse bisector (OB) of the eigenvectors. We infer that SC′-type extensional shear bands form initially parallel to AB and OB and rotate towards the flow plane with progressive deformation, decreasing their inclination relative to the shear zone boundary. AB and OB have significance in the strain field in that they represent orientations of maximum angular strain rate. Thus, planes perpendicular to AB and OB are mechanically favorable for small zones of localized simple shear (shear bands) within the heterogeneous bulk strain of the mylonite. Orientation analysis of populations of SC′-type shear bands may provide a direct, quantitative means of estimating W_k.

1. Introduction

Quantitative structural analysis may provide valuable information regarding the kinematic vorticity of deformation within mylonitic rocks (e.g., Passchier and Simpson, 1986; Passchier, 1987; De Paor, 1988; Wallis, 1995; Beam and Fisher, 1999; Klepeis et al., 1999; Bailey and Eyster, 2003; Giorgis et al., 2003; Law et al., 2004). The relative contributions of the pure and simple shear end-members present during general non-coaxial progressive deformation may be inferred by utilizing the porphyroclast hyperbolic distribution (PHD) method (Simpson and De Paor, 1993, 1997). In addition, the orientations of SC′-type extensional shear bands, measured oblique to the shear zone boundary (Passchier and Trouw, 1998, p. 111), may provide a method of determining bulk kinematic vorticity. The geometric relationship between SC′-type shear bands and their associated flow field has been described differently in the past. Some previous workers have observed and interpreted SC′-type shear band orientations as being coincidental with the direction of maximum angular shear strain rate (i.e., bisecting the acute and obtuse angles between eigenvectors; Simpson and De Paor, 1993, 1997; Klepeis et al., 1999; Law et al., 2004). Conversely, SC′-type shear bands have been interpreted as being oriented parallel to the inclined or unstable eigenvector (Bobyarchick, 1986).

Ductile shear zones within the Cougar Creek Complex (CCC) in the Blue Mountains Province (BMP) of northeastern Oregon and west-central Idaho (Fig. 1) provide an opportunity to evaluate the structural development of quartz-feldspar rocks at mid-crustal levels of the Wallowa island arc system. Mylonitic rocks from the CCC exhibit characteristics which make them suitable for PHD analysis: (1) simple mineralogy; and (2) well-developed and easily recognized deformational textures and fabrics (i.e., the presence of

* Corresponding author.
E-mail address: genekurz@mail.boisestate.edu (G.A. Kurz).

0191-8141/$ – see front matter © 2008 Elsevier Ltd. All rights reserved.
doi:10.1016/j.jsg.2008.04.003

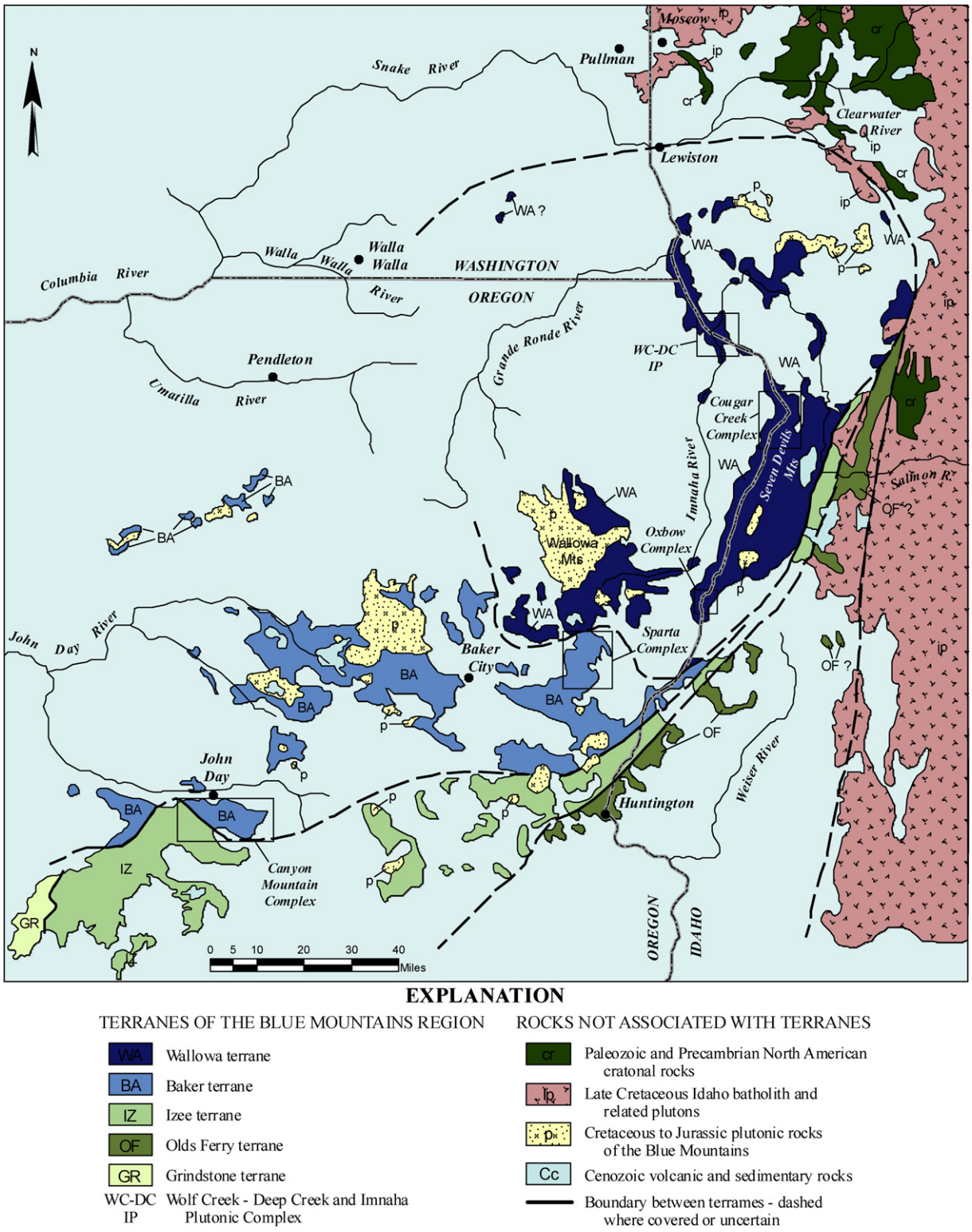

Fig. 1. Blue Mountains province terrane map.Regional geologic map of the Blue Mountains Province, northeastern Oregon, west-central Idaho, and southeastern Washington (After Vallier, 1995).

well-developed porphyroclasts and SC′-type extensional shear bands.

2. Regional geologic context

The CCC is one of five basement complexes within the BMP, and is exposed along a 10-km section of the Snake River within Hells Canyon, between Temperence Creek, Oregon and Pittsburg Landing, Idaho. Similar igneous complexes are located in several parts of the Salmon and Snake River canyons, including: (1) along the Snake River near Oxbow, Oregon, (the Oxbow Complex); (2) near the confluence of the Snake and Salmon rivers (the Wolf Creek–Deep Creek and Imnaha Plutonic Complex); and (3) along the Salmon River between Lucile and White Bird, Idaho (Fig. 1).

Igneous rocks of the CCC are composed of dikes and small stocks with a wide range of bulk compositions, including gabbro, diorite, quartz diorite, tonalite, trondhjemite, and their metamorphosed and deformed equivalents (Vallier, 1995; Kurz, 2001). The CCC is interpreted as the mid-crustal expression of the axial zone related to the Wallowa island arc (Vallier, 1995; Kurz, 2001). Similar igneous complexes have also been documented in the Klamath Mountains of northern California (McFadden et al., 2006).

The CCC is structurally complex and penetratively deformed. Ductile shear zones exhibiting both dextral and sinistral senses of shear were generated within a transpressional tectonic environment experiencing predominant strike-slip to oblique-slip kinematic conditions (Kurz, 2001). Individual shear zones range from one centimeter to several meters in width, strike northeast-southwest, and dip moderately to steeply to both the northwest and southeast. Stretching lineations are sub-horizontal to gently plunging to the southwest and northeast (Kurz, 2001). Mineral assemblages and recrystallization textures within mylonitic rocks indicate greenschist facies conditions of metamorphism at the time of deformation.

3. Methods

3.1. Porphyroclast hyperbolic distribution (PHD) analysis

PHD analysis is based on the rotational behavior of rigid elliptical objects within an actively flowing matrix (Simpson and De Paor, 1993, 1997). During general non-coaxial deformation, the rotational behavior of rigid elliptical porphyroclasts is controlled by the bulk kinematic vorticity (W_k), the axial ratio of the mineral grains (R), and the orientation of their long axes with respect to a fixed reference frame (φ). Three common reference frames are generally used to evaluation vorticity in plastically deformed rocks: (1) the finite strain axes; (2) the infinitesimal strain axes; and (3) the shear zone boundary (Simpson and De Paor, 1997). Commonly, the shear zone boundary and its normal are employed as a reliable frame of reference if it is exposed in the field (Simpson and De Paor, 1997). Axially asymmetric porphyroclasts whose long axes are inclined "downstream" (a downstream dip-direction) of the bulk transport direction at an orientation that falls within the acute angle between the two eigenvectors of the non-coaxial flow field will rotate opposite to the bulk shear sense within a narrowing mylonitic shear zone (Fig. 2; Simpson and De Paor, 1993, 1997). However, as the recrystallization of a porphyroclast progresses, its axial ratio decreases and will eventually stall and not back-rotate further. In thin section it is possible to distinguish forward and backward rotating porphyroclasts, measure their axial ratios (R), and determine the orientation of their long axis relative to the normal of the shear zone boundary (φ). Thus, a data set may be developed containing shape and orientation data that is then plotted on the hyperbolic net (De Paor, 1988). A best-fit hyperbola is plotted asymptotic to the flow plane such that it separates forward and backward-rotating grains (Simpson and De Paor, 1997). The orientation of the inclined eigenvector may then be estimated as the asymptote to the other side of the best-fit hyperbola. The angle v between the two eigenvectors is then used to determine the kinematic vorticity number W_k based on the relationship: $W_k = \cos(v)$ (Fig. 3).

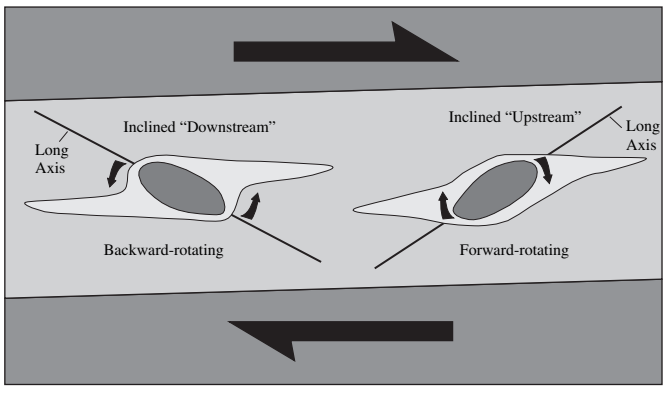

Fig. 2. Schematic diagram of mantled porphyroclasts. Schematic diagram of mantled porphyroclasts that are inclined "upstream" or "downstream" relative to the bulk sense of transport within a narrowing mylonitic shear zone.

3.2. Distinguishing forward and backward-rotated porphyroclasts

Here backward-rotated and forward-rotated porphyroclasts were identified using criteria described by Simpson and De Paor (1993, 1997) for narrowing shear zones. Backward-rotated porphyroclasts are inclined "downstream" relative to the bulk sense of shear and exhibit σ-type asymmetric tails of recrystallized material attached to the broad or long sides of the elongate grain (Figs. 2 and 3; Simpson and De Paor, 1993, 1997). Forward-rotated porphyroclasts were distinguished by (1) approximately equant or spherical δ-grains commonly indicating continuous forward rotation and (2) σ-grains that are inclined "upstream" (an upstream dip-direction) that exhibit recrystallized material attached to their narrow ends (Figs. 2 and 3; Simpson and De Paor, 1993, 1997).

Klepeis et al. (1999) described two variations of backward-rotated grains based on the following criteria: (1) "upstream" or "downstream" inclined porphyroclasts exhibiting a sense of shear contrary to the bulk direction of transport with σ-type tails of recrystallized material attached to either the narrow or broad sides of the grain (β_1 grains; Fig. 3); and (2) σ-type porphyroclasts inclined "downstream" exhibiting asymmetric tails attached to the broad sides of the grain and a rotational direction concurrent with the bulk flow field (β_2 grains; Fig. 3), synonymous with those described by Simpson and De Paor (1993, 1997). In this study, only β_2 grains were observed and employed in PHD analysis, β_1 grains were not identified. Fig. 3 illustrates a variety of observed porphyroclast geometries and related microstructures that may be observed in thin section, as well as, their relationships within the bulk flow field.

3.3. Shear band analysis

The geometry and shear sense of conjugate SC′-type shear band cleavage (Fig. 3) were measured and analyzed in terms of their potential for: (1) determining the non-coaxiality of general shear zones, and (2) illuminating the relationship between the orientation of initial shear band propagation and the direction of maximum angular shear strain rate. The orientation of SC′-type shear bands was determined utilizing the same methods utilized for measuring φ in PHD analysis.

4. Data and observations

4.1. PHD analysis and comparison of shear band orientations

Six mylonite samples from the CCC were analyzed using PHD techniques. Shape and orientation data for measured porphyroclasts and SC′-type shear band geometries are provided as supplementary material or may be requested from the principal author. For each sample the shear zone boundary was discernable and utilized as the reference frame for PHD analysis. In addition, all thin sections were cut perpendicular to foliation and parallel to lineation. Bulk kinematic vorticity numbers determined for the analyzed samples range from $W_k = 0.37$ to $W_k = 0.26$ indicating a significant component of pure shear (76–83% pure shear). W_k

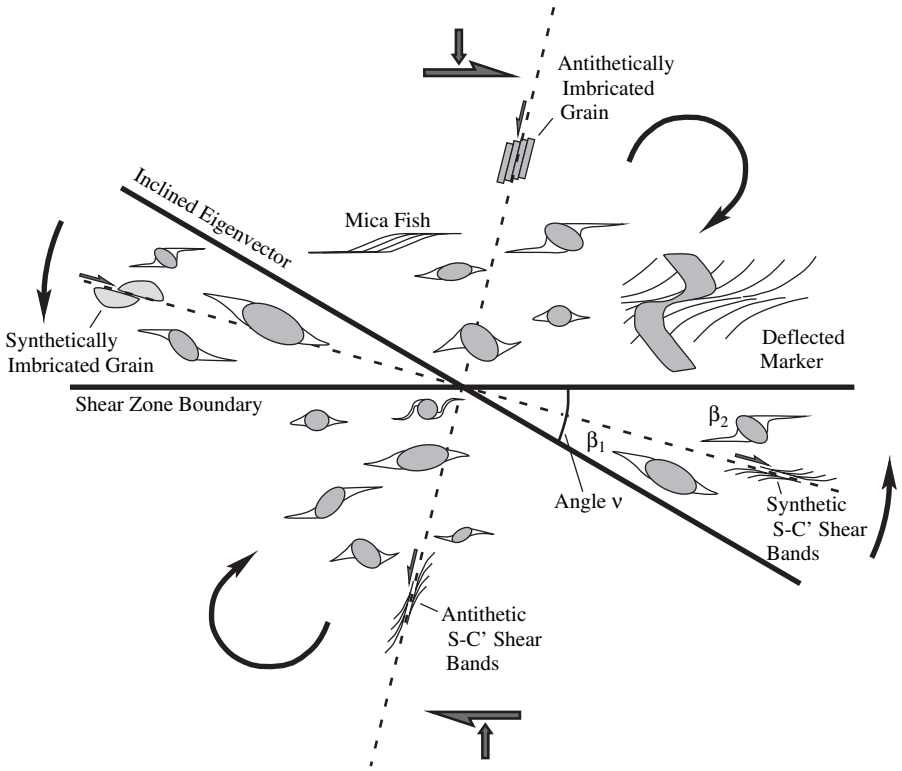

Fig. 3. Schematic diagram of various microstructures. Schematic diagram illustrating fields of forward and backward rotation in a dextral general shear regime, as well as, various micro-structures used in PHD analyses. Dashed lines represent directions of maximum angular shear strain rate. Figure developed from Simpson and De Paor (1993) their Figure 20 and Klepeis et al. (1999) their figure 12.

values for this suite of samples indicate that the unstable eigenvectors are inclined 68° to 75° relative to the shear plane (Fig. 4a–f).

SC′-type shear band orientations were measured within five mylonites to compare their geometry with the flow field determined by PHD analyses. Rose diagrams are combined with PHD plots to illustrate SC′-type shear band orientations and frequency relative to the inferred flow fields of each sample (Fig. 4a–e). Synthetic and antithetic SC′-type extensional shear band cleavages, when present within thin sections, are discontinuous ranging from 0.1 mm to ~1 mm in thickness.

5. Discussion

Lithologies within the CCC provide an opportunity to document and describe the structural evolution of mylonitic rocks, evaluate the initial direction of extensional shear band propagation, and explore whether or not SC′-type shear bands may be used as a qualitative to semi-quantitative means of estimating bulk vorticity. SC′-type shear band orientations were measured within five high strain samples of inferred W_k; and within two, low strain, coarse to medium-grained quartzo-feldspathic aggregates of unknown bulk vorticity.

Measuring SC′-type shear band orientations in the field and during petrographic analysis may be time consuming. This poses the question of how many shear band orientations are needed for confident interpretation. To explore this question, 15 random subsets of synthetic SC′-type shear band orientations for $n = 2$ to $n = 40$ were generated from a single large dataset collected from sample CC-5-27-4 (see Supplementary Material). The mean was determined for each of the 15 random subsets. The standard deviation was determined for each list of means and plotted versus the sample size (i.e., $n = 2$ to $n = 40$). This data illustrates how the standard deviation of the mean decreases with increasing sample size and levels out after the sample size reaches an adequate size, which corresponds to the minimum number of shear bands needed to obtain a representative sample without measuring the entire population of shear bands (Fig. 5). Based on this analysis, a minimum of 30 shear band orientations is recommended to adequately characterize the mean.

5.1. Extensional shear band propagation

The role of shear bands and their geometric relationship to heterogeneous bulk non-coaxial flow is not well understood. Possibilities include formation along the inclined eigenvector (Bobyarchick, 1986) or parallel to AB (Simpson and De Paor, 1993, 1997; Klepeis et al., 1999; Law et al., 2004). Rose diagrams of shear band orientations measured within mylonites have been combined with PHD vorticity illustrations to provide a direct comparison between the geometric relationships of the eigenvectors and shear band positions (Fig. 4a–e). Synthetic shear band orientations within mylonitic rocks of the CCC are oriented either parallel to, or at an angle less than AB. Similarly, antithetic shear bands populations show a range of inclination with a mean inclination lying near OB. These data provide evidence that extensional SC′-type shear bands initially form parallel to AB and OB (Platt and Vissers, 1980; Passchier, 1984; Wilson, 1984; Simpson and De Paor, 1993, 1997; Klepeis et al., 1999; Law et al., 2004).

Shear bands that are inclined at an angle less than AB and OB are the result of either: (1) rotation towards the shear zone boundary during progressive non-coaxial flow; (2) formed under heterogeneous non-steady-state conditions and/or varying bulk vorticity; or (3) formed during separate episodes of deformation. Assuming a steady-state general flow regime, synthetic and antithetic extensional shear bands are expected to rotate towards the stable eigenvector and away from AB and OB throughout progressive non-coaxial deformation. Nucleation of shear bands at an orientation parallel to AB and OB is supported by the data presented here.

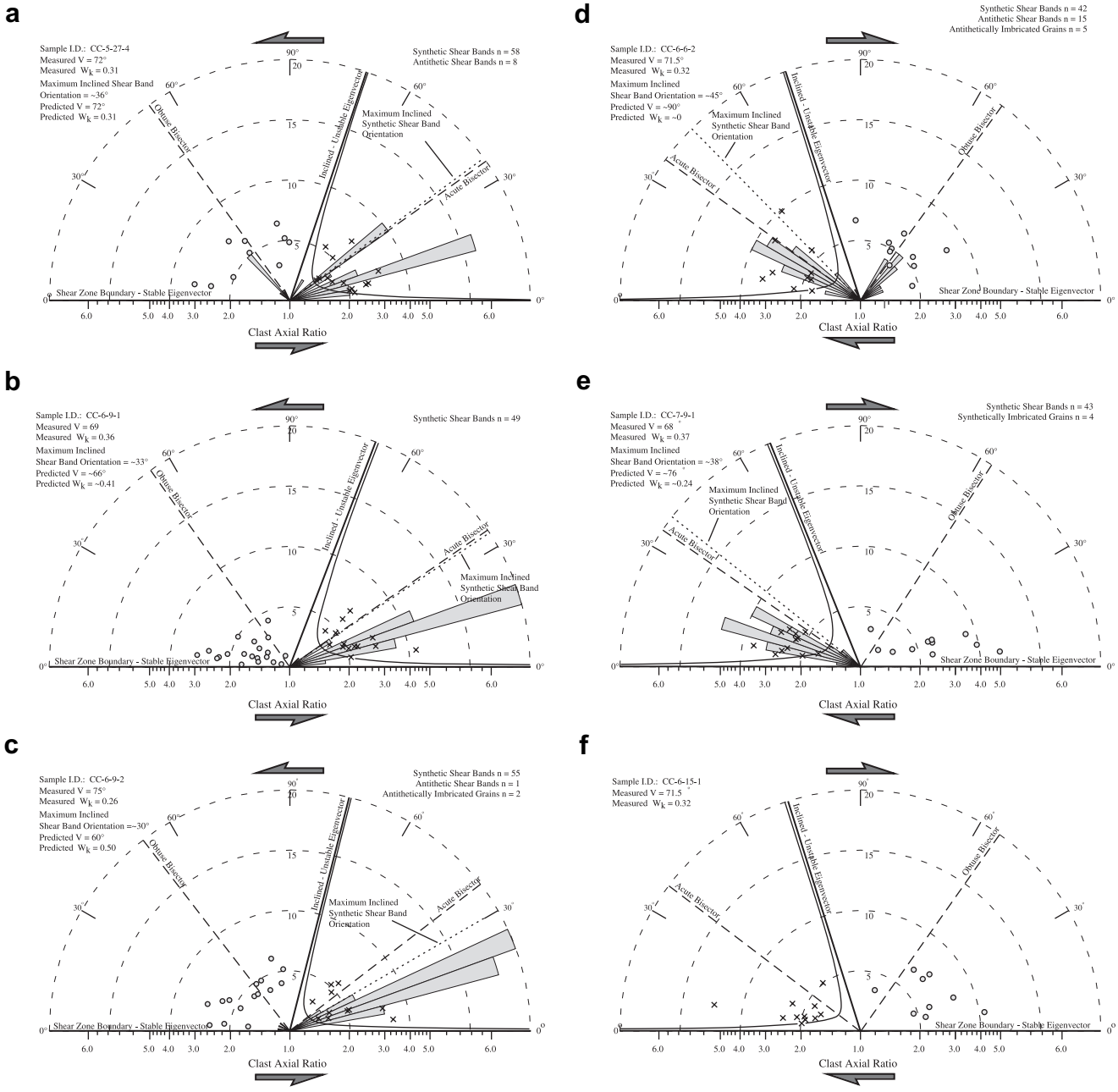

Fig. 4. PHD diagrams. PHD diagrams for mylonitic rocks from the CCC. Rose diagrams generated from orientation data for synthetic and antithetic SC'-type shear bands and other related structures such as synthetically and antithetically imbricated mineral grains are combined with PHD diagrams. This combination is meant to illustrate geometric relationships and frequency distributions of shear band orientations relative to the inferred flow field determined from PHD analyses. Porphyroclast axial ratio data relates to the scale along the base of each diagram. Annular dashed half-circles measure shear band frequency data associated with rose diagrams. Dotted lines indicate the maximum inclination of synthetic SC'-type shear band within two standard deviations of the mean and are used to estimate kinematic vorticity. Black X's represent plotted backward-rotated porphyroclasts while gray-filled circles depict plotted forward-rotated porphyroclasts.

5.2. Estimation of bulk vorticity utilizing SC′-type extensional shear bands

Provided that SC′-type shear bands initiate at an orientation parallel to AB and OB, these structures may be utilized to estimate the non-coaxiality of general shear within rocks deformed by crystal-plastic mechanisms. However, the majority of samples in this study display a range of shear band orientations of shear bands, with mean values frequently observed at an angle less than that of AB and OB. This observation may reflect the rotation of these material lines towards the stable eigenvector throughout progressive strain. Because of the rotational behavior of shear bands after formation, the arithmetic mean of a set of measured SC′-type shear band orientations will likely underestimate the coaxial component of the bulk vorticity. Assuming steady-state vorticity during progressive deformation, the most steeply inclined shear bands may provide the best direct estimate of AB and OB in that shear bands at this orientation may not have been significantly rotated.

Given that material lines such as SC′-type extensional shear bands will rotate towards the stable eigenvector or shear zone boundary in rocks recording larger amounts of accumulated strain (Hanmer and Passchier, 1991; Simpson and De Paor, 1993), it is reasonable to believe that SC′-type shear band orientations within low strain rocks will have potentially undergone lesser amounts of rotation. Thus, at an early stage of deformation, the mean shear

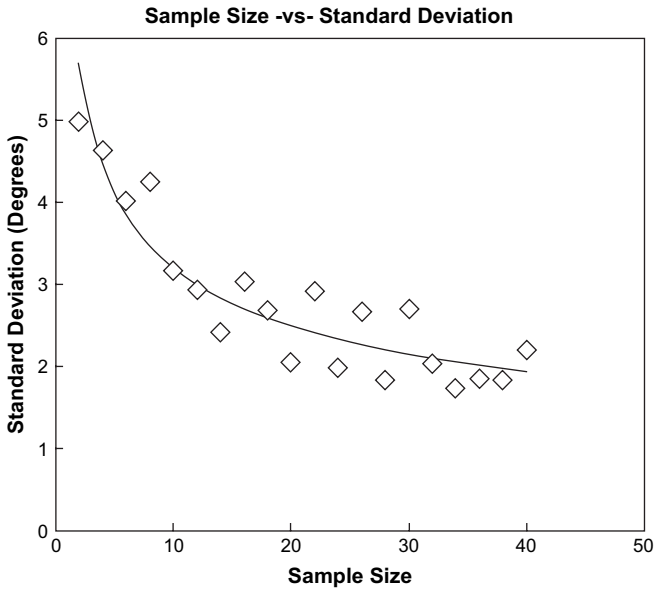

Fig. 5. Sample size versus standard deviation. Sample size versus standard deviation illustrates how the standard deviation of a mean shear band orientation decreases with increasing sample size. An optimum sample size was chosen where the slope of the curve begins to flatten near n = 30 to 40.

band orientation within a low strain rock will be more representative of the initial position in which they formed (Fig. 6).

Mylonites from the CCC may provide an example of this behavior. SC′-type shear band orientations were used to estimate W_k from five mylonites from the CCC, estimated values were then compared with W_k values inferred from PHD analysis. Estimated values for bulk vorticity within high strain rocks were determined by utilizing the most steeply inclined shear band orientation within ± two standard deviations of the mean in order to eliminate outliers. Generally, the most steeply inclined shear band orientation overestimated the coaxial component of bulk vorticity as compared to values discerned from PHD analysis (Fig. 4a–e). Two samples overestimated the pure shear component relative to inferred W_k values (Fig. 4d and e), however, shear bands from two other samples gave estimates for the angle v within ~3° of their graphically determined v angles (Fig. 4a and b). Shear band cleavage orientations from a fifth mylonite underestimated W_k (Fig. 4c). Estimated bulk vorticity derived from shear band analysis range from $W_k \approx 0.50$ to $W_k \approx 0$. These estimates corresponding to a range of v angles of 60° to 90° which relate to pure shear components of ≈67% to ≈100%.

5.3. Estimating bulk vorticity in lower strain rocks

Petrographic investigation of deformational textures and fabrics in two coarse to medium-grained quartz-feldspar aggregates from the CCC of unknown vorticity indicate a lesser amount of dynamic

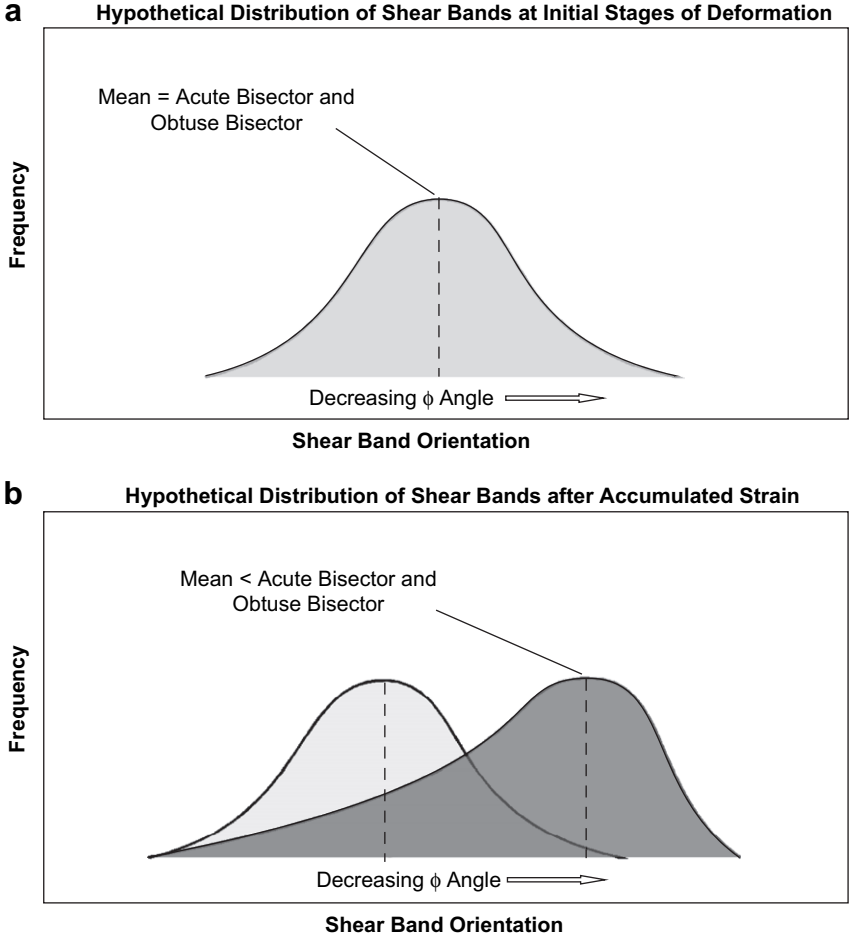

Fig. 6. Distribution of shear band orientations. (a) Schematic distribution of shear band orientation which have undergone only a small amount of strain. At this stage of deformation shear bands have not accumulated enough strain to rotate away from AB and OB. The arithmetic mean of a set of measured shear bands may provide a reasonable estimate of the bulk vorticity. (b) Distribution of shear band orientations after accumulated strain (Dark Gray). Notice that the mean of this sample has been skewed to the right, away from AB and OB. Here, the most steeply inclined shear band orientation may provide the best direct estimate of bulk vorticity of a rock mass that has been plastically deformed under steady-state general noncoaxial flow.

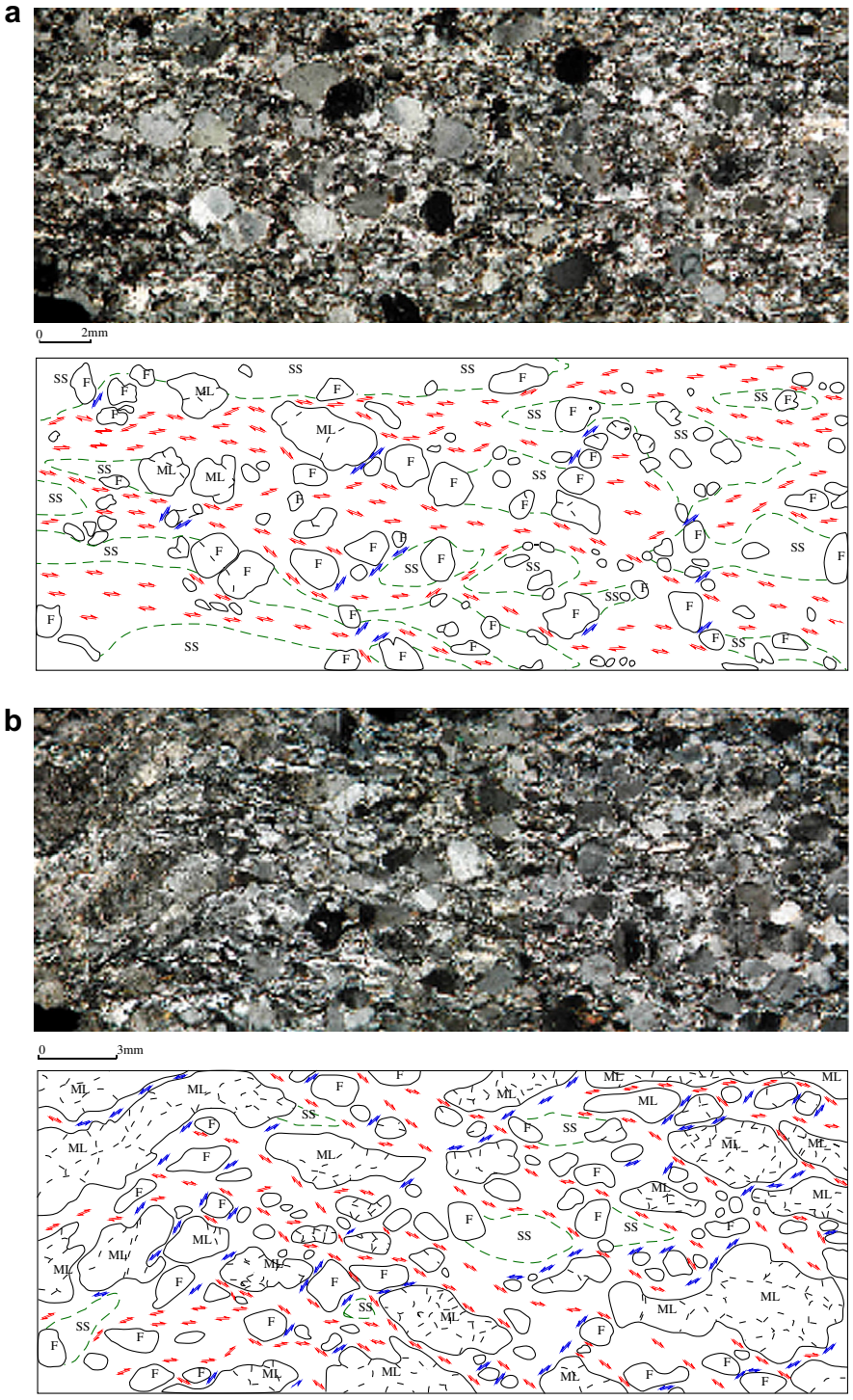

Fig. 7. Composite images of samples CC-6-30-1 and CC-6-4-1. Composite image of samples CC-6-30-1 (a) and CC-6-4-1 (b), examples of weakly recrystallized coarse to medium-grained quartz-feldspar aggregates. An anastomosing network of quartz-rich, micro-scale shear zones have accommodated the majority of the strain within the rock mass.

recrystallization relative to samples analyzed by PHD techniques. These two samples exhibit moderately to well-defined SC′-type shear bands that form an anastomosing network of quartz dominated microshear zones and enclose large microlithons of feldspar (Fig. 7a and b). Because these coarse to medium-grained quartz-feldspar aggregates appear to have undergone comparatively smaller amounts of strain, the arithmetic mean of shear band orientations has been used to estimate bulk vorticity.

Within these two coarse-grained samples there is definite interaction between large feldspar grains that may influence the orientation of shear bands in a manner that is not representative of the bulk vorticity. This may invalidate conclusions regarding the use of shear band orientations to estimate bulk vorticity, however, not all observed shear bands were associated with grain to grain interaction.

Rose diagrams generated from measured shear band orientations of these two samples reveal a close geometrical relationship with those that were produced for samples where the bulk vorticity is inferred from PHD analyses (Fig. 8a and b). Synthetic shear bands measured within mylonite CC-6-30-1 are inclined at an average

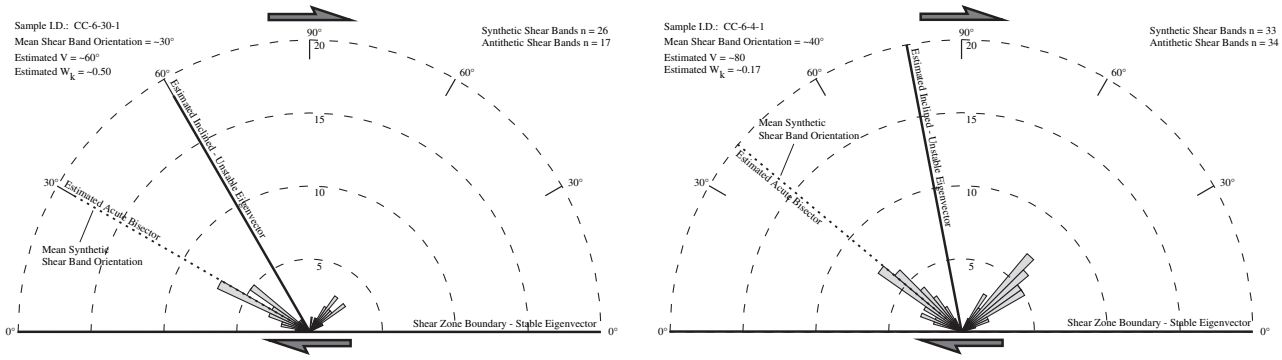

Fig. 8. Half rose diagrams for samples CC-6-4-1 and CC-6-30-1. Rose diagrams illustrating SC'-type shear band orientations from samples CC-6-30-1 (a) and CC-6-4-1 (b). Dashed line represents the estimated orientation of AB.

angle of ~30°, relative to the shear zone boundary (Fig. 8a). Assuming that this average orientation roughly bisects the angle v, the estimated vorticity is approximately $W_k = 0.50$, where $v = 60°$. Shear band orientations for mylonite CC-6-4-1 are, on average, inclined at a slightly higher angle relative to the boundary of the shear zone than those measured within sample CC-6-30-1. The mean inclination (φ) of shear bands within sample CC-6-4-1 is ~40° indicating v=80° (Fig. 8b). The estimated bulk vorticity corresponding to this mean inclination is $W_k = 0.17$. The estimated values of bulk vorticity for these two quartz-feldspar aggregates are similar to values determined for high strain samples, assuming that the deformation within these coarse-grained samples was produced during the same episode of dextral shearing as other right-lateral mylonites. Thus, the mean orientation of a sample of SC′-type shear bands within lower strain rocks may provide reasonable estimates of the orientations of AB and OB.

6. Conclusions

Analyses combining PHD methods (Simpson and De Paor, 1993, 1997) and measured orientations of SC′-type extensional shear bands suggest the following: (1) SC′-type extensional shear bands initially propagate at an orientation parallel to AB and OB (Simpson and De Paor, 1993, 1997; Klepeis et al., 1999; Law et al., 2004); (2) progressive strain following shear band formation produces rotation of shear bands towards the flow plane, generating a mean inclination that is less than the orientation of AB and OB, and therefore underestimates the coaxial component of the general flow regime; (3) the most steeply inclined shear band orientation provides the best direct estimate of W_k within high stain rocks; and (4) shear band orientations within weakly recrystallized rocks may record bulk vorticity more accurately than those measured in high-strain mylonites. Ultimately, SC′-type extensional shear bands provide a means of broadly characterizing the non-coaxiality of general shear.

Acknowledgements

The authors would like to thank the Boise State University Geosciences department for the facilities to conduct our research and writing. Funding, in part, was provided by the Boise State University Geosciences Student Research Grant (Will and Rose Burnham Fund). The authors would like to specifically acknowledge Dr Richard D. Law of the Department of Geosciences at Virginia Tech; this manuscript has greatly benefited from his careful reviews and criticisms. The principal author would like to thank his wife and family for their encouragement and support during my career in geology.

Appendix A. Supplemental material

Supplementary information for this manuscript can be downloaded at doi: 10.1016/j.jsg.2008.04.003.

References

Bailey, C.M., Eyster, E.L., 2003. General shear deformation in the Pinaleno Mountains metamorphic core complex, Arizona. Journal of Structural Geology 25, 1883–1893.
Beam, E.C., Fisher, D.M., 1999. An estimate of kinematic vorticity from rotated elongate porphyroclasts. Journal of Structural Geology 21, 1553–1559.
Bobyarchick, A.R., 1986. The eigenvalues of steady flow in Mohr space. Tectonophysics 122, 35–51.
De Paor, D., 1988. R_f/φ strain analysis using an orientation net. Journal of Structural Geology 10, 323–333.
Giorgis, S., Tikoff, B., McClelland, W.C., 2003. Removal of the Mid-Cretaceous Idaho Batholith by the crustal-scale, western Idaho shear zone. Geological Society of America Abstracts with Programs 35 (6), 473.
Hanmer, S., Passchier, C.W., 1991. Shear-sense indicators: a review. Geological Survey of Canada Paper 90-17, 72.
Klepeis, K.A., Daczko, N.R., Clarke, G.L., 1999. Kinematic vorticity and tectonic significance of superposed mylonites in a major lower crustal shear zone, northern Fiordland, New Zealand. Journal of Structural Geology 21, 1385–1405.
Kurz, G.A., 2001, Structure and geochemistry of the Cougar Creek Complex, Northeastern Oregon and West-Central Idaho. MS thesis, Boise State University, Boise, ID, 248 pp.
Law, R.D., Searle, M.P., Simpson, R.L., 2004. Strain, deformation temperatures, and vorticity of flow at the top of the Greater Himalayan Slab, Everest Massif, Tibet. Journal of Structural Geology 161, 305–320.
McFadden, R.R., Snoke, A.W., Barnes, C.G., 2006. Structural and petrologic evolution of the Bear Peak intrusive complex, Klamath Mountains, California. In: Snoke, A. W., Barnes, C.G. (Eds.), Geological Studies in the Klamath Mountains Province. California and Oregon: A Volume in Honor of William P, 410. Geological Society of America Special Paper, Irwin, pp. 333–355.
Passchier, C.W., 1984. The generation of ductile and brittle shear bands in a low-angle mylonite zone. Journal of Structural Geology 6, 273–281.
Passchier, C.W., 1987. Stable positions of rigid objects in non-coaxial flow – a study in vorticity analysis. Journal of Structural Geology 9, 679–690.
Passchier, C.W., Simpson, C., 1986. Porphyroclast systems as kinematic indicators. Journal of Structural Geology 8, 831–843.
Passchier, C.W., Trouw, R.A.J., 1998. Microtectonics, second corrected reprint. Springer-Verlag, Berlin, 289 pp.
Platt, P.P., Vissers, R.L.M., 1980. Extensional structures in anisotropic rocks. Journal of Structural Geology 2, 397–410.
Simpson, C., De Paor, D.G., 1993. Strain analysis in general shear zones. Journal of Structural Geology 15, 1–20.
Simpson, C., De Paor, D.G., 1997. Practical analysis of general shear zones using the porphyroclast hyperbolic distribution method: an example from the Scandinavian Caledonides. In: Sengupta, S. (Ed.), Evolution of Geological Structures in Micro- to Macro-scales. Chapman and Hall, London, pp. 169–184.
Vallier, T.L., 1995. Petrology of Pre-Tertiary igneous rocks in the Blue Mountains Region of Oregon, Idaho, and Washington: implications for the geologic evolution of a complex island arc. In: Vallier, T.L., Brooks, H.C. (Eds.), The Geology of the Blue Mountains Region of Oregon, Idaho, and Washington: Petrology and Tectonic Evolution of Pre-Tertiary Rocks of the Blue Mountains Region. US Geological Survey Professional Paper 1438, pp. 125–210.
Wallis, S., 1995. Vorticity analysis and recognition of ductile extension in the Sanbagawa belt, SW Japan. Journal of Structural Geology 17, 1077–1093.
Wilson, C.J.L., 1984. Shear bands, crenulations and differentiated layering in ice-mica models. Journal of Structural Geology 6, 303–319.